An X-Ray Absorption Edge Detector for High-Resolution Measurement of Undulator Effective *K*-Parameter

B. Yang* and J. N. Galayda[†]

* Argonne National Laboratory, 9700 South Cass Avenue, Argonne, IL 60439
[†] Stanford Linear Accelerator Center2575 Sand Hill Road, Menlo Park, CA 94025

Abstract. The spectrum of angle-integrated undulator radiation displays a sharp edge at every harmonic photon energy. A technique utilizing this feature to measure minute changes in K-parameters of an undulator in a free-electron laser has been proposed. To date, this technique requires the use of crystal monochromators as bandpass filters whose energy centroid depends on the incident angle of the x-ray beam. In this work we propose to use the absorption edge of an appropriate element as an energy-selective detector whose response is truly independent of the angle of the x-ray beam, and hence independent of electron beam direction and emittance. We will discuss the basic design concept of the detection system and illustrate its projected performance with computer simulations.

INTRODUCTION

The Linear Coherent Light Source (LCLS) is a linac-based x-ray free-electron laser (XFEL) [1]. The x-ray beam is generated by a high-quality electron beam traversing through an undulator over 130 meters in length. The undulator is divided into 33 segments, with each 3.4-m-long segment having 112 ($N = 112$) magnetic periods that are 3.0 cm long. To obtain lasing, the LCLS design requires stringent control of the *K*-values of the undulator segments, 3.5000 ± 0.0005, a tolerance of $\Delta K/K = \pm 1.5 \times 10^{-4}$. This requirement will be met initially by an offline magnetic measurement facility. However, since the longitudinal wakefield causes the energy of the electron bunch to decrease as it travels down the undulator chamber, a beam-based measurement technique is desirable to help taper the *K*-values to compensate for the energy loss. The beam-based measurement technique may also be used to evaluate and track gradual degradation of the magnets after their exposure to the radiation environment.

Several techniques have been proposed to measure the effective *K* using the spontaneous radiation of the undulator. The angle-integrated measurements appear to have a robust spectral feature against beam jitters, especially when they are used for relative measurements, i.e., for comparison of one undulator segment with a standard one [2]. To date, these techniques require the use of crystal monochromators as bandpass filters, and their energy centroid depends on the incident angle of the x-ray

beam. In this work we propose to use the absorption edge of an appropriate element as an energy-selective detector whose response is truly independent of the angle of the x-ray beam, and hence independent of electron beam direction and emittance.

Table 1 shows electron energy value for the first undulator harmonic x-ray energy of LCLS undulator that coincides with the cobalt or nickel K-absorption edge. In this work, we will use cobalt as our detector film to illustrate the design concept. We will also show how to reduce signal background using standard x-ray techniques and demonstrate the expected performance of the detector using computer simulations.

TABLE 1. LCLS X-ray energy

Electron energy (GeV)	x-ray energy (eV)	Notes
13.64	8266	Maximum nominal operating energy
13.173	7709	Cobalt K-edge
13.695	8333	Nickel K-edge

DETECTOR DESIGN AND PERFORMANCE ESTIMATE

Figure 1 shows a schematic of the detector. A cobalt metal foil absorber is used as the detector media, and a PIN photon diode is used to collect Co K-fluorescence photons from the foil. The following efforts were made to reduce background levels.

- A set of tungsten slits is used to control the acceptance aperture of the detector. To maintain a constant angular aperture, the slits will be adjusted according to the distance between the undulator and the detector. An x-ray camera downstream is used to keep the beam centered in the aperture and verify its size.
- A multilayer-coated mirror is used to reduce the background due to the higher harmonics of the undulator radiation. As we will see later, the reduction ratio is over 100.
- The thickness of the Co film is chosen to be 80% of an absorption length above the K-edge, enhancing useful photon flux without increasing background significantly.
- The PIN diode is mounted facing the metal film normally so the solid angle of the PIN diode is not sensitive to the location of the fluorescing atom. Furthermore specularly reflected low-energy photons will be sent away from the diode.
- An optional filter may be inserted between the absorber film and the detector, so only high-energy fluorescence photons from the K-shell will reach the detector.
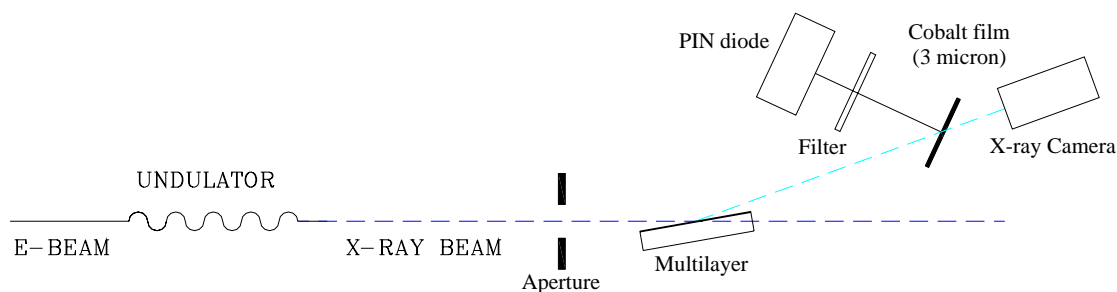

FIGURE 1. Schematic of the K-edge detector.

Response Function of the Detector System

Our absorption spectrum data of cobalt came from two sources: most of the data is from the NIST database via the program XOP [3] except the data from 7680 eV to 8500 eV, when the spectrum near the edge was measured [4] and normalized to the NIST database. The following observations can be made from the data (Fig. 2A).

- In the region above and near the K-edge, about 13% of the x-ray absorption events are due to excitation of L-shell electrons. These events results in fluorescence x-ray photons in the range of $800 - 900$ eV with very low yield ($< 2\%$) and hence do not contribute to the K-fluorescence signal. Only a portion of $\eta_K \sim 87\%$ of absorption events is useful.
- Of all K-shell events for cobalt, $\sim 50\%$ result in fluorescence photons, $Y_K \sim 0.5$ [5].
- The total thickness of the detector foil is about one absorption length above the K-edge. It is thus only $\sim 1/8$ of absorption length below the edge and is nearly transparent to the fluorescent x-ray photons, $K_{\alpha1}$, $K_{\alpha2}$, and K_β.
- For all fluorescence photons, the PIN diode's collection efficiency is $\Omega_D/4\pi$, where Ω_D is the solid angle of the detector with respect to the beam spot on the foil.

Summarizing the above discussion, the number of photons collected by the diode per electron bunch is given by

$$S(\omega_1) = q\frac{\Omega_D}{4\pi}\int F(\omega;\omega_1)R(\omega)d\omega,\tag{1}$$

where q is the bunch charge in nC, $F(\omega;\omega_1)$ is the undulator flux through the aperture per nC, $R(\omega) = \eta_K Y_K R_M(\omega)\left[1 - e^{-\mu(\omega)t}\right]$ is the response function of the detector system, $\omega_1 = 2\gamma^2\omega_u/(1 + K^2/2)$ is the first harmonic photon energy, $R_M(\omega)$ is the reflectivity of the mirror, $\mu(\omega)$ is the attenuation coefficient, and t is the beam path length in the film. Figure 2B shows the calculated reflectivity curve of a multilayer optic with 50 pairs of tungsten (1.5 nm) and silicon (1.0 nm) layers. Figure 2C shows the response function $R(\omega)$ along with the undulator radiation spectrum. The intensity of the fluorescence photon signal is roughly proportional to the overlap area of the two spectra. The sensitivity of the detector system to changes in undulator effective K is measured by gain factors G_ω, G_γ and G_K defined here,

$$\frac{\Delta S(\omega_1)}{S(\omega_1)} = G_\omega\frac{\Delta\omega_1}{\omega_1} = G_\gamma\frac{\Delta\gamma}{\gamma} = -G_K\frac{\Delta K}{K}, \quad G_\gamma = 2G_\omega = \left(1 + \frac{2}{K^2}\right)G_K.\tag{2}$$

Varying the first harmonic energy ω_1 in Eq. (1) and assuming a good acceptance angle $\Omega_D/4\pi = 0.03$, we calculated the changes of fluorescence photon flux. The results are shown in Fig. 3. Operating with the first harmonic energy ω_1 slightly higher than ω_K, $\tau = N\frac{\omega_1 - \omega_K}{0.36\cdot\omega_1} = 1$ and $\omega_1 = 7740$ eV, we obtain a good signal level without sacrificing much gain. Here the gain is 365, and for $\Delta K/K = \pm10^{-4}$, the detector signal

changes by $\Delta S(\omega_1)/S(\omega_1) = \mp 3.6\%$, which can be easily measured by average electronics. Hence the proposed detector is very sensitive for $\Delta K/K$ measurements.
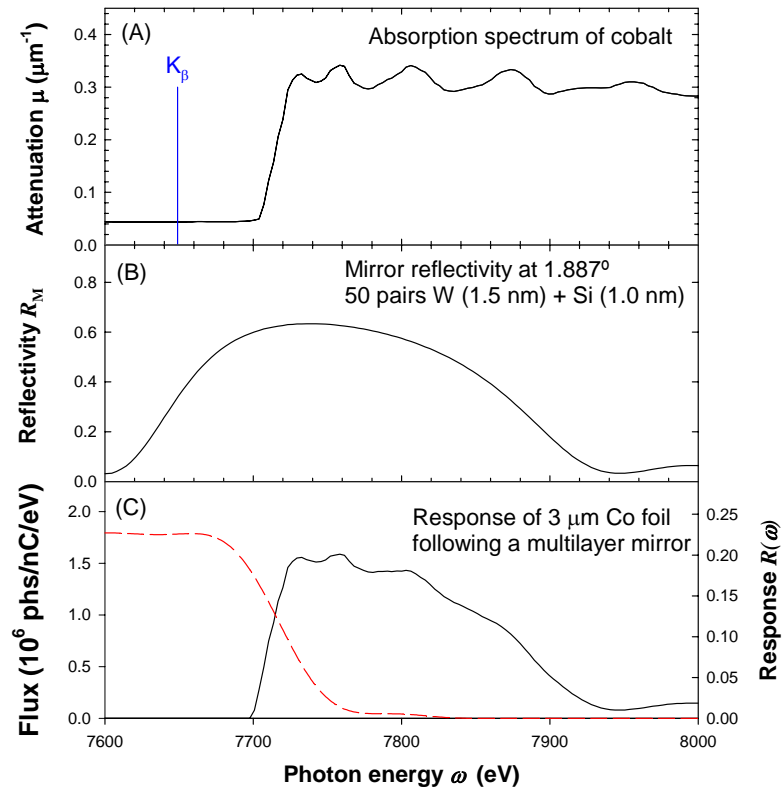

FIGURE 2. (A) Attenuation spectrum of cobalt. (B) Calculated multilayer optic reflectivity spectrum. (C) Solid curve shows the K-shell response function of the detector system, which vanishes below the K-edge. Dashed line shows the angle-integrated undulator radiation spectrum.
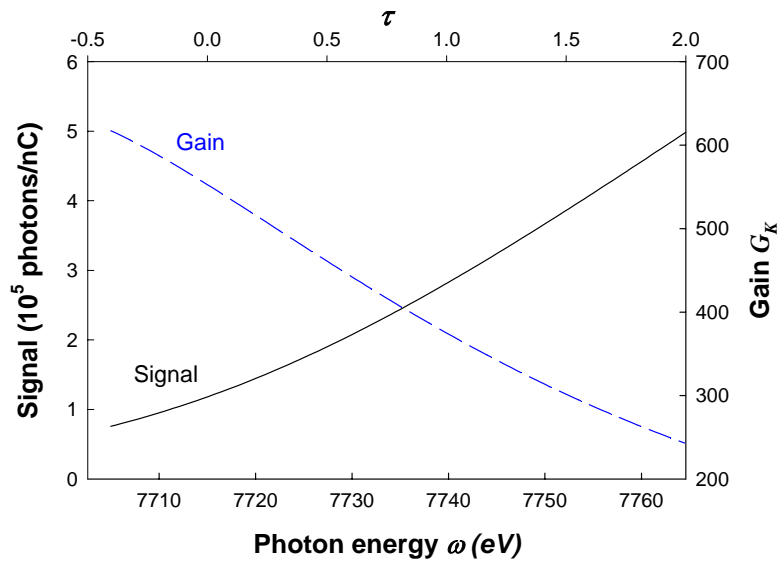

FIGURE 3. Solid curve shows the fluorescence signal collected by the PIN diode. Dashed line shows the gain factor for effective K.

Background and Instrument Effects

In the previous section, we evaluated Eq. (1) only in the Co K-edge region. Absorption of higher energy x-rays are not sensitive to the change in undulator K-parameter and hence contribute mainly to background. To estimate this background, we use calculated properties of the LCLS undulator (Fig. 4A) and multilayer mirror (Fig. 4B), and known absorption data (Fig. 4C) to evaluate Eq. (1) one harmonic at a time. The results are shown in Fig. 4D. We can see that the background is ~ 1% of the signal intensity when we use the multilayer mirror. The background would be over two orders of magnitude stronger if we do not use the mirror.
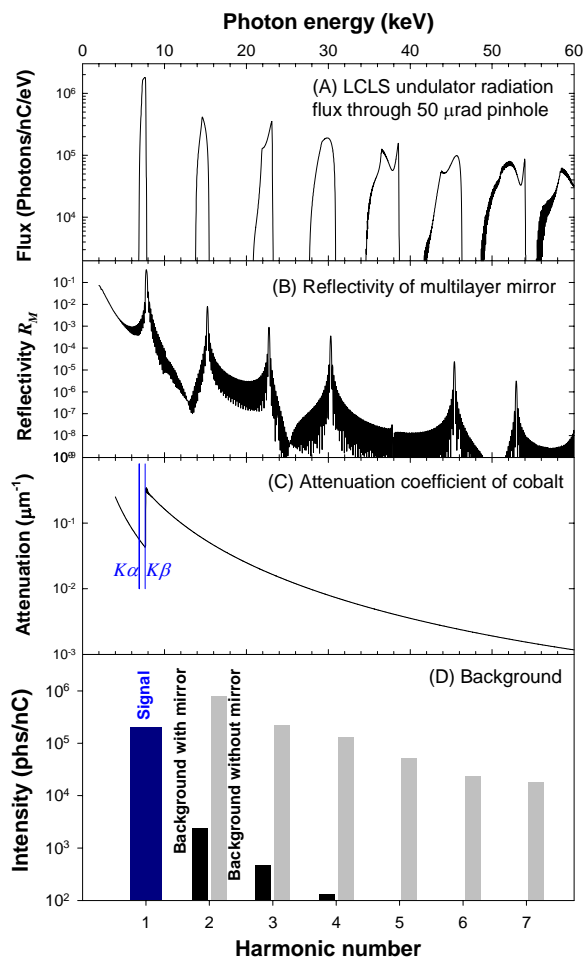

FIGURE 4. (A) Spectrum of spontaneous radiation of LCLS undulator through a 50 µrad aperture. (B) Multilayer mirror reflectivity spectrum. (C) Attenuation spectrum of cobalt. (D) Comparison of signal intensity (n = 1) with higher harmonic background when a multilayer mirror is used (left) and when it is not used (right).

Since the reflectivity of the multilayer depends on the incident angle, the signal level also depends on the incident angle. From Fig. 5A, we can see that this signal reaches a peak around 1.887º, where changes in signal intensity are less than 1% for an angle deviation of ±50 µrad. Hence the intensity change caused by the x-ray beam divergence of 8 µrad and electron beam angle jitter of 0.5 µrad will be less than 0.1%.

Next we consider the variation of detector solid angle due to a varying location of the fluorescence source. For a square diode with a width $2d$ and a distance L from the Co foil, it extends a full angle of $2\theta_0 = 2\arctan(d/L)$ in both transverse planes. If the source moves a distance x horizontally, the detector's horizontal acceptance angle changes to $2\theta = \arctan[(d+x)/L] + \arctan[(d-x)/L]$, corresponding to a relative change $\dfrac{\theta_0 - \theta}{\theta_0} = -\dfrac{\tan\theta_0 \cos^4\theta_0}{\theta_0}\left(\dfrac{x}{L}\right)^2$. If we use a 18 mm square diode, e.g., Hamamatsu S3204, and assume that the beam spot can move up to 2.5 mm from center (the inner radius of the LCLS undulator chamber), we need a distance $L \geq$ 22 mm to limit the intensity variations to less than 1%. At this distance, the diode extends a solid angle $\Omega_D/4\pi \sim 0.05$ with respect to the beam spot.

While the independence of the location of fluorescing atoms guarantees that the signal is independent of the incoming x-ray beam size and position, the jitter of bunch charge q and electron energy γ, however, is a totally different matter. The bunch charge is proportional to the spontaneous photon flux, and the effect of energy jitter is magnified due to Eq. (2). To compensate for these effects, we record q and γ shot by shot and fit the result to the following expression (Fig. 5B),

$$\ln\frac{QS_{\exp}}{q_{\exp}} = \ln D + a_1\delta + a_2\delta^2, \quad (\delta = \frac{\gamma - \gamma_0}{\gamma_0}), \tag{3}$$

where γ_0 is the nominal electron energy and Q is quantum efficiency of the PIN diode. The y-intercept of the fitted curve gives us the true measurement data D. This procedure is an accurate and efficient way of "averaging" multi-shot data.
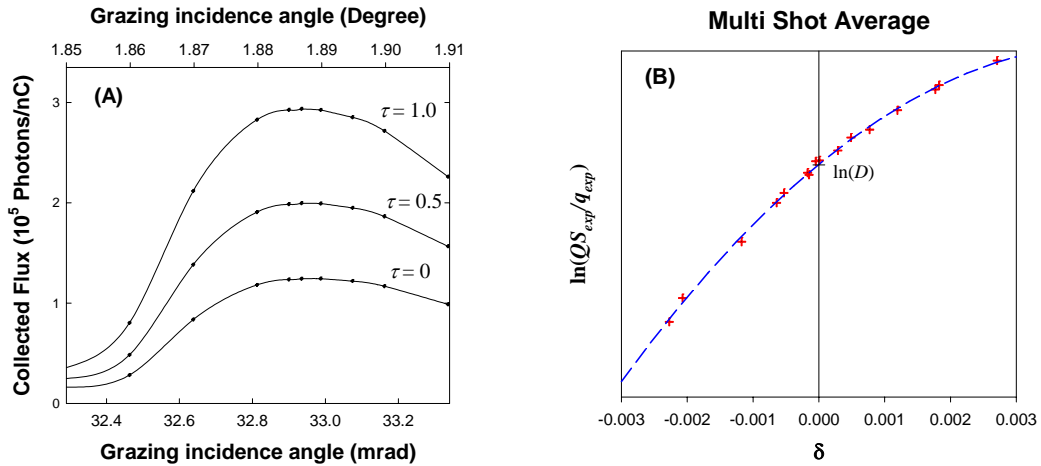

FIGURE 5. (A) The expected detector signal as a function of incidence angle to the multilayer-coated mirror, for three electron energies. (B) Deriving data from multi-shot measurements using curve fit.

USE THE DETECTOR TO SET UP UNDULATORS

Since the longitudinal wakefield depends on bunch length and charge, it is desirable to use the operational bunch parameters to set up the undulator. To perform our

simulation, we assume a nominal bunch charge q = 0.2 nC with an rms jitter of 10% and a measurement accuracy of 0.5%. We also assume an rms electron energy jitter of 0.1% with a measurement accuracy of 2×10^{-5}, and a detector quantum efficiency Q = 0.25. Finally, a statistical noise $\sqrt{QS(\omega_1)}$ is added to the detected number of photons before performing the fit shown in Fig. 5B. The effect of the added noise can be seen from the scatter of data points in the figure.

Step 1: Center undulators vertically. After beam-based alignment of electron trajectory, the first step is to make sure that the trajectory is on the magnetically neutral plane of the undulators. The magnetic field and effective K change with the electron's vertical coordinates y,

$$\frac{K(y) - K(0)}{K(0)} = \frac{\alpha_y}{2}\left(\frac{y}{\lambdabar_u}\right)^2 , \qquad (4)$$

where $\lambdabar_u = \lambda_u/2\pi$ is given by the undulator's magnetic period. α_y is a constant of the order of one and is determined by the geometry of the magnetic structure. For LCLS undulators, a vertical displacement of 70 μm of the entire undulator results in a change of $\Delta K/K \sim 10^{-4}$.

In the simulated vertical scan, we allow the electron trajectory to move vertically in the undulator for ± 75 μm, thus changing the K-value according to Eq. (4) (α_y = 1 for simplicity). Using 32 bunches per measurement, the scan yields data shown in Fig. 6A. Statistical analysis shows rms error of the measured position of the neutral plane to be less than 2 μm, well within the tolerance of ± 35 μm.

Step 2: Setup detector and electron beam. One of the 33 undulator segments will be a standard undulator with its field strength independent of its horizontal position. Its properties should be measured often, so we have high confidence in its effective K (denoted as K_0) and in its field qualities. First we roll this undulator into position and then adjust the electron energy so that the signal D reaches a predetermined setting D_0. In these simulation studies, $D_0 = 1.20 \times 10^5$ counts/nC. Next, we scan the mirror angle to obtain a curve (Fig. 5A) and set the mirror at the peak of the curve. Iterate these two steps until the detector signal D attains D_0 at the peak of the mirror scan. Derive the experimental gain factor G_γ from the slope of the fitted curve in Fig. 5B and obtain the gain factor G_K using Eq. (2) for later use.

Step 3: Horizontal undulator scan. The LCLS undulators use a 4.5-mrad canted magnetic structure for fine and reproducible setting of the magnetic field. For a full horizontal displacement of 6.25 mm, the effective K changes 0.6%. In this step, we roll in one undulator segment at a time, set the detector acceptance aperture to 30 μrad, and center the aperture using the x-ray camera. Figure 6B shows the simulated scan data $D(x_u)/D_0$, where x_u is the undulator displacement from its geometrical center position.

Since one scan takes 1 – 3 minutes per undulator, this curve should be measured and stored regularly, e.g., when routine beam-based alignment is performed. A reduction of magnetic strength would cause the curve to shift up. The dashed line in Fig. 6B shows data from a 2×10^{-4} uniform field reduction across all poles. Since the

radiation damage to undulator magnets is usually localized near the beam pipe, changes in the field may also be somewhat localized. The dashed-dot line in Fig. 6B shows the data for a maximum of 4×10^{-4} field reduction in a region 3 mm in rms width. If we record the scan data of a new undulator segment, $D_1(x_u)$, on its first day and routinely perform the same scan periodically, we will be able to detect changes in the undulator field, whether uniformly or localized, from changes in measured signal strength and its spatial distribution, at a level of $\Delta K/K \sim 10^{-4}$ or better.

Step 4: Set undulator effective K. After measuring the undulator segments and archiving the field data, each undulator can be set to its final position according to desired K-value distribution, uniform or tapered. The K-value of each undulator segment gives the target photon counts,

$$D(K) = D_0 \left(1 - G_K \frac{K - K_0}{K_0} \right), \qquad (5)$$

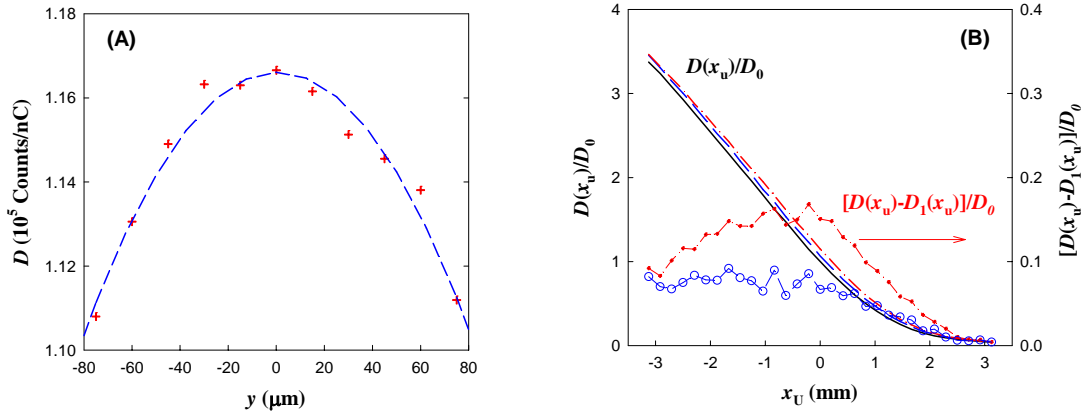and the desired horizontal position can be derived from the measured curve in Fig. 6B.

FIGURE 6. (A) Vertical electron trajectory scan shows effective-K variation away from the magnetic neutral plane. Each point uses 32×0.2 nC electron bunches. (B) Horizontal undulator scans: solid curve is for an LCLS undulator with a nominal cant. Dashed curve is for an undulator with 2×10^{-4} uniform field reduction. Dash-dot curve is for an undulator with a localized damage with an rms radius of 3 mm and a 4×10^{-4} field reduction at its peak region. The differences of the signals between the weakened and standard undulators are shown in a magnified scale. Spatial characteristics of the damage can be seen from the spatial distributions.

SUMMARY AND ACKNOWLEDGMENTS

We proposed a novel K-edge absorption-based detection system for characterizing undulator effective K. We showed that it is insensitive to beam transverse properties and has a good potential for high-resolution measurement and routine observation of undulators in an XFEL at a level of better than 10^{-4}. Further studies are warranted to explore more details in its performance.

REFERENCES

1. J. Arthur et al., "LCLS Conceptual Design Report," SLAC-R-593, http://www-ssrl.slac.stanford.edu.
2. B. Yang, "High-Resolution Undulator Measurements Using Angle-Integrated Spontaneous Radiation," Proc. PAC 2005, 2342-2344 (2005). http://www.jacow.org.
3. M. Sanchez del Rio and R. J. Dejus "XOP: Recent Developments," SPIE proceedings Vol. 3448, pp.340-345 (1998).
4. Arild Moen and David G. Nicholson, "X-ray Absorption Spectroscopic Studies at the Cobalt K-Edge on a Reduced Al_2O_3-Supported Rhenium-Promoted Cobalt Fischer-Tropsch Catalyst," Chem. Mater., 9, 1241-1247 (1997).
5. M. O. Krause, "Atomic Radiative and Radiationless Yields for K and L Shells," J. Phys. Chem. Ref. Data 8, 307 (1979).